Event-Triggered H_∞ Filtering for Cyber–Physical Systems Against DoS Attacks

Xiang Sun, Zhou Gu, *Member, IEEE*, Dong Yue, *Fellow, IEEE*, and Xiangpeng Xie, *Member, IEEE*

***Abstract*—This article mainly focuses on the problem of resilient H_∞ filtering for cyber–physical systems (CPSs) subject to denial-of-service (DoS) attacks and sensor saturation. A new event-triggered mechanism (ETM) considering both DoS attacks and limited network bandwidth is put forward to guarantee the secure performance of the filter. Under this mechanism, inherent periodical transmission attempts are generated during DoS active periods, by which the latest measurement output of the system can be successfully transmitted to the filter after the end of the DoS attack; while during DoS sleep periods, the ETM degenerates into a traditional one. Furthermore, a valid DoS attack model is proposed to further characterize the following two scenarios occurring between adjacent sampling instants: 1) the end of the DoS attack and 2) both the start of the DoS attack and the end of the DoS attack. Sufficient conditions for designing the secure filters of CPSs against DoS attacks are achieved by using the piecewise Lyapunov–Krasovskii functional approach. Finally, the validity of our designed approach is manifested by an illustration of quarter-vehicle suspension systems (SSs).**

***Index Terms*—Cyber–physical systems (CPSs), event-triggered mechanism (ETM), filter design, valid denial-of-service (DoS) attacks.**

I. INTRODUCTION

RECENT achievements of research attracting constant attention on cloud computing, wireless communication, and hardware technologies have promoted the development of cyber–physical systems (CPSs).

Owing to the introduction of the network in CPSs, some challenging issues may arise in the research of CPSs, such as the issues of cyber security [1], [2], [3], [4], [5], limited bandwidth [6], [7], [8], and networked delay [9], [10], [11]. For example, the secure estimation and control problem for CPSs under adversarial attacks was investigated in [12]. An event-triggered control with a dynamic relative threshold strategy was designed in [13] for active seat suspension systems (SSs) to reduce the network burden of the actuator and controller. In [14], the event-triggered H_∞ controller considering the distributed channel delay was designed for the networked control systems.

It is noteworthy that the filtering problem over sensor networks for CPSs has been a fascinating research hotspot in the field of signal processing [15], [16], [17]. In [18], the Lagrange multiplier method is utilized to achieve the local finite impulse response filter gain for wireless sensor networks. A distributed set-membership filtering problem for a class of time-varying multirate systems under the round-Robin scheduling over sensor networks was studied in [19]. In the traditional filtering issue, signal transmission is commonly assumed to be continuous. However, with the enormous advancements of sensing, embedded computing, and wireless communication technology, the processing signal is transmitted via wireless networks by time-triggered transmission schemes on digital platforms nowadays. Although the time-triggered transmission scheme has a wild application due to the convenience of analysis and design, it is unsuitable on the problem of the perspective of power consumption and limited network bandwidth. In this respect, the event-triggered mechanism (ETM) is an efficient way in reducing the network resource since the packets with the system information are selectively released only when the predesigned ETM-based condition is invoked [20], [21]. In [22], for saving the bandwidth and increasing the maximum allowable time delay under a nonideal network, an event-triggered H_∞ filtering for cloud-aided semi-vehicle SSs was provided.

It is noticed that the specification between the lower data release rate and better system performance is contradicted. To further reduce the data releasing rate and ensure system performance, the state-of-the-art ETM has been proposed in recent years. For example, in [23], an adaptive ETM was investigated for the decentralized H_∞ filtering of nonlinear interconnected systems, wherein the threshold is designed to be adaptively adjusted with the system state. Tian and Peng [24] addressed the memory-based event-triggered controller design for power systems considering random deception attacks, wherein some historical triggered data were utilized in the proposed ETM such that both the network bandwidth and the control performance can be ensured simultaneously.

In addition, owing to the effect of the cyber attacks to CPSs on the real physical world, the security filtering for CPSs with bandwidth-constrained communication network is worthy of further study. The denial-of-service (DoS) attack as a typical attack mode has attracted wide attention in

Manuscript received 10 July 2022; accepted 24 October 2022. Date of publication 8 November 2022; date of current version 17 April 2023. This work was supported in part by the National Natural Science Foundation of China under Grant 62273183, Grant 62022044, and Grant 62103193 and in part by the Postgraduate Research & Practice Innovation Program of Jiangsu Province, China, under Grant KYCX20_0855. This article was recommended by Associate Editor E. Usai. *(Corresponding author: Zhou Gu.)*

Xiang Sun and Zhou Gu are with the College of Mechanical and Electronic Engineering, Nanjing Forestry University, Nanjing 210037, China (e-mail: gzh1808@163.com; sx032812@163.com).

Dong Yue and Xiangpeng Xie are with the Institute of Advanced Technology, Nanjing University of Posts and Telecommunications, Nanjing 210023, China (e-mail: medongy@vip.163.com; xiexiangpeng1953@163.com).

Color versions of one or more figures in this article are available at https://doi.org/10.1109/TSMC.2022.3218023.

Digital Object Identifier 10.1109/TSMC.2022.3218023

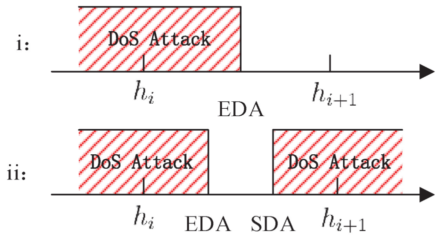

Fig. 1. Two scenarios of DoS attacks.

CPSs [25], [26], [27]. In [28], a general DoS model was introduced where its frequency and duration are constrained, wherein the frequency and duration of DoS attacks are explicitly characterized. The stability of the system can be maintained on the pretext of the state-feedback controller. The resilient ETM-based control problem for CPSs subject to DoS attacks was investigated assuming that the control input is zero in DoS active periods in [29] and [30]. A similar formulation was considered in [31], where the authors studied the H_∞ filtering problem for CPSs under nonperiodic DoS attacks. However, the following two scenarios (shown in Fig. 1) are neglected in the existing published literature: 1) the end of the DoS attack occurs within a sampling period and 2) the end of the DoS attack and the start of the follow-up DoS attack occur in a same sampling period. Therefore, this article aims to establish a new communication strategy utilizing the ETM considering the above scenarios in the filtering error systems subject to DoS attacks.

On another research frontier, the sensor saturation caused by physical/technological restrictions in providing limited amplitudes of signals has been researched in the recent literature [32], [33], [34]. The performance of the system could be severely degraded if the sensor saturation is not appropriately handled [35]. Consequently, the critical issue in this topic is to seek a reasonable algorithm that can fully utilize the available information and meet the required performance. In [36], a resilient H_∞ filter was developed to ensure the mean-square stability subject to randomly distributed delay and sensor saturation. The filtering problem for continuous-time linear systems subject to sensor saturation is studied in [37]. Therefore, the influence of the sensor saturation should be considered in the filtering problem of the real CPSs.

Inspired by the previous deliberation, this article investigates H_∞ filtering for CPSs with sensor saturation subject to DoS attacks. The main contribution addressed in this work is as follows.

1) A novel DoS attack model is put forward, in which two scenarios are considered in what follows: a) the end of the DoS attack occurs within a sampling period and b) the end of the DoS attack and the follow-up DoS attack occur in a same sampling period. From the natural effect of the DoS attack on the system, a new definition of "*valid*" DoS attack (VDA) that can perfectly cover the above two scenarios is proposed.
2) A new ETM using the VDA model is established. Under this communication strategy, the ETM generates inherent periodical transmission attempts during the period of the VDA till the VDA ends, that is, the latest packet containing the system information can be successfully transmitted over the network after the end of the VDA. Therefore, the resilient H_∞ performance of the filter for CPSs can be guaranteed, and the network communication load can be reduced based on the proposed communication strategy.

The remainder of this article is arranged as follows. Section II presents the system model, the communication strategy against DoS attacks, and the filtering error system. In Section III, the H_∞ filtering for CPSs with the sensor saturation against DoS attacks is designed. A numerical example is provided to indicate the effectiveness of our proposed method in Section IV. The conclusion is drawn in Section V.

Notations: We denote the following notations in this article. sym$\{X\}$ represents the sum of X and X^{T}; diag$\{\cdot\}$ stands for a diagonal matrix. $\mathbb{N}$ is the set of natural numbers and $\mathbb{N}_0 := \mathbb{N} \cup 0$.

II. Problem Statement

The main task of this study is to design an event-triggered H_∞ filter for CPSs with sensor saturation against DoS attacks.

A. System Model

1) Plant: Consider the physical plant described by the linear time-invariant system as follows:

$$\begin{cases} \dot{x}(t) = Ax(t) + B\omega(t) \\ z(t) = Ex(t) \\ y(t) = Cx(t) \end{cases} \tag{1}$$

where $\omega(t)$ denotes the disturbance; and $y(t)$ and $z(t)$ denote the measurement output by the sensor and the output of the physical plant to be estimated, respectively.

Due to physical/technological restrictions, the system's output in (1) is limited by sensor saturation. The saturation function of signals can be defined as $\mathrm{sat}(\xi) = \mathrm{sgn}(\xi)\min\{|\xi|, \bar{\xi}\}$, where $\bar{\xi}$ denotes the threshold of the sensor saturation function. Therefore, we have

$$\mathrm{sat}(y(t)) = \left[\mathrm{sat}(y_1(t)), \mathrm{sat}(y_2(t)), \ldots, \mathrm{sat}(y_m(t))\right]^{\mathrm{T}}, m \in \mathbb{N} \tag{2}$$

where

$$\mathrm{sat}(y_i) = \begin{cases} \bar{y}_i, & y_i(t) > \bar{y}_i \\ y_i(t), & -\bar{y}_i \le y_i(t) \le \bar{y}_i, i = 1, 2, \ldots, m \\ -\bar{y}_i, & y_i(t) < -\bar{y}_i. \end{cases} \tag{3}$$

Similar to [38], the real system's output in (1) with sensor saturation can be represented by

$$\tilde{y}(t) = \mathrm{sat}(y(t)) = y(t) - \vartheta(y(t)) \tag{4}$$

where $\vartheta(y(t)) = [\vartheta(y_1(t)), \vartheta(y_2(t)), \ldots, \vartheta(y_m(t))]^{\mathrm{T}}$ and $\vartheta(y(t))$ is a nonlinear function satisfying

$$\vartheta^{\mathrm{T}}(y(t))\vartheta(y(t)) \le \epsilon y^{\mathrm{T}}(t)y(t) \tag{5}$$

for positive scalar ϵ, where $\epsilon = \max\{\epsilon_1, \epsilon_2, \ldots, \epsilon_m\}$, $\epsilon_i \in (0, 1)$ and $\epsilon_i \ge (1 - [\bar{y}_i/(|y_i(t)|\max)])^2$, where $|y_i(t)|\max$ is the maximum amplitude of output $y_i(t)$.

2) Filter: The dynamic filtering system can be represented as follows:

$$\begin{cases} \dot{x}_f(t) = A_f x_f(t) + B_f y_f(t) \\ z_f(t) = C_f x_f(t) \end{cases} \tag{6}$$

where $x_f(t)$ denotes the state of the filter, $z_f(t)$ and $y_f(t)$ denote the output and input of the filter, respectively; and A_f, B_f, and C_f are filter gains.

B. Communication Strategy Against DoS Attacks

For filters, both the ETM and DoS attacks can cause the missing measurement. The difference between them is that the former discards unnecessary information actively to relieve the load of the network, while the latter loses data indiscriminately within the DoS active period, which reduces the performance of filters. To ensure the H_∞ performance of the filtering error system against DoS attacks and save the network bandwidth, we will propose a new model combining both the ETM and DoS attacks in this part.

Referring to a general DoS model in [28], $\mathcal{A}(t_1, t_2)$ and $\mathcal{S}(t_1, t_2)$ are the active and sleep period of DoS attacks in time interval $[t_1, t_2]$, respectively. They are defined as follows:

$$\mathcal{A}(t_1, t_2) = \bigcup_{n\in\mathbb{N}} D_n \cap [t_1, t_2] \tag{7}$$

$$\mathcal{S}(t_1, t_2) = [t_1, t_2] \setminus \mathcal{A}(t_1, t_2) \tag{8}$$

where $D_n = [d_n, d_n + \tau_n)$ represents the interval of the nth DoS attack, of a duration $\tau_n \geq 0$, over which the filter cannot receive packets in the DoS period. d_n with $d_1 \geq 0, n \in \mathbb{N}$ denotes the start of the nth DoS attacks. In this study, the DoS attack is assumed to be technologically detectable.

Considering the fixed sampling measurement output, the following two scenarios of DoS attacks may occur in practice, as is shown in Fig. 1. For further clarifying this issue, an example with these two scenarios is presented in Fig. 2, where h_i denotes the ith sampling instant, from which we know that:

1) The end of the DoS attack occurs within a sampling period, for example, the end of the first DoS attack is at the instant $d_1 + \tau_1$, which is between the sampling instants h_2 and h_3. Since the sensor of CPS cannot release the sampling packets within the time interval $[d_1 + \tau_1, \rho_1 + \partial_1)$, we define $[\rho_1, \rho_1 + \partial_1)$ as a VDA period rather than $[d_1, d_1 + \tau_1)$ under this scenario.
2) The end of the DoS attack and the follow-up DoS attack occur in a same sampling period, for example, the end of the DoS attack at $d_2 + \tau_2$ and the follow-up DoS attack at d_3 in Fig. 2 are occurred in the same sampling period $[h_6, h_7)$. From the perspective of data transmission, the sampling packets cannot be released within the time interval $[d_2 + \tau_2, d_3]$ and $[d_3 + \tau_3, h_{10})$. Therefore, the second VDA period can be described by the time interval $[\rho_2, \rho_2 + \partial_2)$.

Remark 1: As shown in Fig. 2, due to the existence of a sampling interval, the impact time of the DoS attack will be longer than the actual attack time. For example, the end of the first DoS attack is $d_1 + \tau_1$, however, the end of the first VDA is $\rho_1 + \partial_1$.

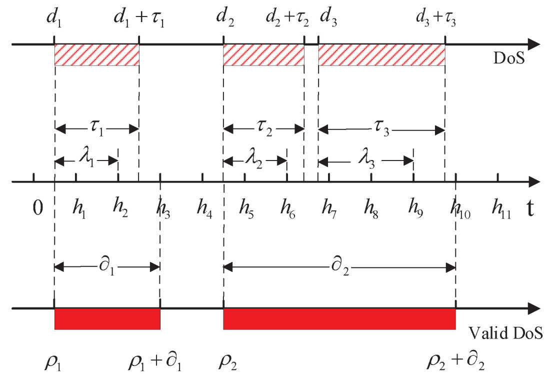

Fig. 2. Example with the scenarios in Fig. 1.

Besides, for clearly expressing the VDA, we denote the set of series sampling instants within D_n by $\mathcal{H}_n = \{i | i \in \mathbb{N}, h_i \in D_n\}$. In Fig. 2, $\mathcal{H}_1 = \{1, 2\}$, $\mathcal{H}_2 = \{5, 6\}$ and $\mathcal{H}_3 = \{7, 8, 9\}$, and let $\lambda_n = h_s - d_n$, $s = \max_{i\in\mathcal{H}_n} i$.

It is known that the start of the DoS attack as discussed in scenario 2) is not the start of VDAs, such as d_3 in Fig. 2. Therefore, we redefine the start of VDAs as

$$\rho_{m+1} = \inf\{d_n \geq \rho_m | d_n > d_{n-1} + \lambda_{n-1} + h\} \tag{9}$$

with $\rho_1 = d_1$.

Then, one can obtain the mth VDA period as

$$\check{\mathcal{A}}_m = [\rho_m, \rho_m + \partial_m) \tag{10}$$

with the duration $\partial_m = \sum_{\substack{n\in\mathbb{N} \\ \rho_m \leq d_n < \rho_{m+1}}} |A_n \backslash A_{n+1}|, A_n = [d_n, d_n + \lambda_n + h)$.

On these grounds, $\check{\mathcal{S}}_m = [\rho_m + \partial_m, \rho_{m+1}) \cup [0, \rho_1)$ defines the mth sleep period of VDAs in the interval $[\rho_m, \rho_{m+1}) \cup [0, \rho_1)$. For convenience, we define $\rho_0 + \partial_0 = 0$. Therefore, $\check{\mathcal{S}}_m$ is rewritten as

$$\check{\mathcal{S}}_m = \big[\rho_m + \partial_m, \rho_{m+1}\big), \ \ m \in \mathbb{N}_0 \tag{11}$$

and $\sum_{m=0}^{\infty} \check{\mathcal{A}}_m \cup \check{\mathcal{S}}_m = [0, \infty)$.

Considering VDAs, one can express the ETM as

$$t_{k+1}h = t_k h + \inf\{\varpi \mid \phi(t) \geq 0\} \tag{12}$$

with $\phi(t) = e^{\mathrm{T}}(t)\Omega e(t) - (1 - \zeta(t_\varpi h))\delta \tilde{y}^{\mathrm{T}}(t_k h)\Omega \tilde{y}(t_k h)$, where $e(t) = \tilde{y}(t_k h) - \tilde{y}(t_\varpi h)$, $t_\varpi h = t_k h + \varpi h$, $\zeta(t_\varpi h) \in \{0, 1\}$ is a detection signal of DoS attacks and δ is a given constant parameter.

Remark 2: If the attack belongs to the active period of VDAs, the detection signal $\zeta(t_\varpi h)$ turns to be 1, that is, $\phi(t) > 0$ is always maintained during the VDA period. Therefore, the event at each sampling time is triggered during VDA, which implies $t_{k+1}h = t_k h + h$. These triggered packets with inherent sampling period h cannot be transmitted to the filter from the network owing to DoS attacks. However, the latest measurement output can be successfully transmitted to the filter after the VDA ends. This behavior is called a "periodical transmission attempt." Once the attack is under the sleep period of VDAs with $\zeta(t_\varpi h) = 0$, the ETM in (12) can be regarded as a general ETM as in [20].

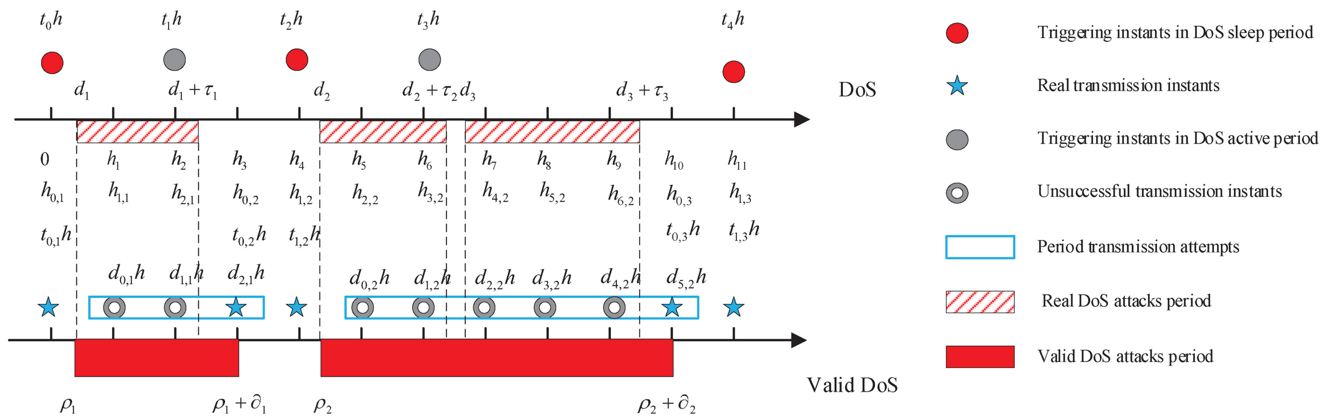

Fig. 3. Real releasing instants.

To ensure the packet at the end of VDA can be successfully transmitted over the network, (10) and (11) are redefined as

$$\begin{aligned}\bar{\mathcal{A}}_m &= [\rho_m, \rho_m + \partial_m]\\ \bar{\mathcal{S}}_m &= (\rho_m + \partial_m, \partial_{m+1}).\end{aligned} \tag{13}$$

Remark 3: From the ETM in (12), one knows that if the instant $\rho_m + \partial_m$ belongs to the VDA period, the periodical transmission attempt works. Thus, the packet at this instant can be successfully transmitted over the network due to the end of the DoS attack in practice.

According to the ETM in (12) and the model of VDAs in (13), we redefine the real transmitting instant $t_{k,m+1}h$ as

$$\begin{aligned}t_{k,m+1}h \in &\left\{t_{\varpi}h \text{ satisfying } (12) | t_{\varpi}h \in \bar{\mathcal{S}}_m\right\}\\ &\cup\{\rho_m + \partial_m\}\end{aligned} \tag{14}$$

where $m, \varpi \in \mathbb{N}_0$, $t_{0,m+1}h = \rho_m + \partial_m$.

Remark 4: In [29] and [31], the following two scenarios were neglected: 1) the end of the DoS attack occurs within a sampling period and 2) the end of the DoS attack and the start of the follow-up DoS attack occur in the same sampling period, which is considered in this article. Besides, different from the assumption that the end of the DoS attack should occur at the sampling instant and the event generator artificially transmit the latest data to the filter in [30], the proposed event-triggered condition and the VDA model in this work can avoid the above-mentioned problems and ensure that the filter can receive the latest packet from the plant after the DoS attack ends.

C. Filtering Error System

Before designing a filtering error system considering DoS attacks, we give the following definitions:

$$\begin{aligned}h_{0,m+1} &= \rho_m + \partial_m\\ q_a(m) &= \sup\left\{q \in \mathbb{N}_0 | h_{q,m+1} < \rho_{m+1} + \partial_{m+1}\right\}\\ q_s(m) &= \inf\left\{q \in \mathbb{N}_0 | h_{q,m+1} \geq \rho_{m+1}\right\}\\ s(m) &= \sup\left\{s \in \mathbb{N}_0 | d_{s,m+1}h \leq \rho_{m+1} + \partial_{m+1}\right\}\\ k(m) &= \sup\left\{k \in \mathbb{N}_0 | t_{k,m+1}h < \rho_{m+1}\right\}\end{aligned}$$

where $h_{0,m+1}$ and $h_{q_a(m),m+1}$ represent the first sampling instant (FSI) and the last sampling instant (LSI) within the time interval $[\rho_m + \partial_m, \rho_{m+1} + \partial_{m+1})$, respectively; $h_{q_s(m),m+1}$ and $d_{s(m),m+1}h$ represent the FSI and the LSI during the time interval $[\rho_m, \rho_m + \partial_m)$, respectively; and $t_{k(m),h}$ represents the last triggering instant within the time interval $[\rho_m + \partial_m, \rho_{m+1})$. For example, in Fig. 3, when m equals to 1, we have $q_a(1) = 6$; $q_s(1) = 2$; $s(1) = 5$; and $k(1) = 1$.

Define $\mathcal{G}_{s,m} = [d_{s,m+1}h, d_{s+1,m+1}h)$ and $\mathcal{R}_{k,m} = [t_{k,m+1}h, t_{k+1,m+1}h)$, where $s \in \{0, 1, \ldots, s(m)\}$, $k \in \{0, 1, \ldots, k(m)\}$. Then, it yields that the active and sleep period of VDAs are $\sum_{s=0}^{s(m)} \mathcal{G}_{s,m} \cap \bar{\mathcal{A}}_m$ and $\sum_{k=0}^{k(m)} \mathcal{R}_{s,m} \cap \bar{\mathcal{S}}_m$.

Combining the real transmitting instant $t_{k,m+1}h$ in (14) and the above definitions, we reformulate $\phi(t)$ in (12) by

$$\phi(t) = \begin{cases}\phi_s(t), t \in \mathcal{R}_{k,m} \cap \bar{\mathcal{S}}_m\\ \tilde{e}^{sT}_{m+1}(t)\Omega\tilde{e}^{s}_{m+1}(t), t \in \mathcal{G}_{s,m} \cap \bar{\mathcal{A}}_m\end{cases} \tag{15}$$

where

$$\begin{aligned}\phi_s(t) &= e^{kT}_{m+1}(t)\Omega e^{k}_{m+1}(t) - \delta\tilde{y}^{\mathrm{T}}\big(t_{k,m+1}h\big)\Omega\tilde{y}\big(t_{k,m+1}h\big)\\ e^{k}_{m+1}(t) &= \tilde{y}\big(t_{k,m+1}h\big) - \tilde{y}\big(t_{k,m+1}h + \varpi h\big)\\ \tilde{e}^{s}_{m+1}(t) &= \tilde{y}\big(d_{s,m+1}h\big) - \tilde{y}\big(d_{s,m+1}h + \varpi h\big).\end{aligned}$$

Correspondingly, $d_{s+1,m+1}h = d_{s,m+1}h + h$, and $t_{k+1,m+1}h = t_{k,m+1}h + \varpi_n h$ with $\varpi_n = \inf\{\varpi | \phi(t) \geq 0, t \in \mathcal{R}_{k,m} \cap \bar{\mathcal{S}}_m\}$.

Considering VDAs and the ETM in (15) yields that

$$y_f(t) = \begin{cases}\tilde{y}\big(t_{k,m+1}h\big), & t \in \mathcal{R}_{k,m} \cap \bar{\mathcal{S}}_m\\ 0, & t \in \mathcal{G}_{s,m} \cap \bar{\mathcal{A}}_m.\end{cases} \tag{16}$$

Then, define $\eta(t) = t - t_{k,m+1}h - \varpi h$ for $t \in \mathcal{R}_{k,m} \cap \bar{\mathcal{S}}_m$, one can obtain that

$$\tilde{y}\big(t_{k,m+1}h\big) = e^{k}_{m+1}(t) + \tilde{y}(t - \eta(t)). \tag{17}$$

To get a compact format, we denote $\mathcal{F}_{g,m} = [t_{g,m}, t_{3-g,m+g-1})$, where

$$t_{g,m} = \begin{cases}\rho_m + \partial_m, & g = 1\\ \rho_{m+1}, & g = 2\end{cases} \tag{18}$$

and $\chi(t) = \mathrm{col}\{x(t), x_f(t)\}$, $e_f(t) = z(t) - z_f(t)$.

Then combining (4), (6), and (15)–(17), we replace the filter in (6) for $t \in \mathcal{F}_{g,m}$, $g \in \{1, 2\}$ as a switched system below

$$\begin{cases}\dot{\chi}(t) = \tilde{A}_g\chi(t) + \tilde{B}\omega(t) + \tilde{C}_g e^{k}_{m+1}(t)\\ \quad + \tilde{C}_g y(t - \eta(t)) - \tilde{C}_g\vartheta(y(t - \eta(t)))\\ e_f(t) = \tilde{E}_g\chi(t)\end{cases} \tag{19}$$

where

$$\tilde{A}_g=\begin{bmatrix}A & 0\\ 0 & A_{fg}\end{bmatrix},\tilde{B}=\begin{bmatrix}B\\0\end{bmatrix},\tilde{C}_1=\begin{bmatrix}0\\B_f\end{bmatrix}$$
$$\tilde{E}_g=\begin{bmatrix}E & -C_{fg}\end{bmatrix},\tilde{C}_2=0.$$

The main target of this article is to design the secure filter in (6) based on our proposed communication strategy such that the system (19) is exponential stable with H_∞ norm bound γ.

III. Main Results

The networked filtering system with the sensor saturation subject to DoS attacks is formulated as a switched system in Section II. To guarantee the exponential stability of the system (19) with H_∞ norm bound γ, sufficient conditions are presented in Theorem 1. In Theorem 2, we will derive the gains of the filter.

Before that, we define $m(\tilde{t}_1,\tilde{t}_2)$ and $\mathcal{U}(\tilde{t}_1,\tilde{t}_2)$ as the number and the union of VDAs, respectively. Then, the following assumptions are first given.

Assumption 1 (DoS Frequency) [28]: There exists $\kappa_f>0$ such that

$$m(\tilde{t}_1,\tilde{t}_2)\le(\tilde{t}_2-\tilde{t}_1)/\kappa_f \tag{20}$$

for all $t\in[\tilde{t}_1,\tilde{t}_2]$ with $0\le\tilde{t}_1<\tilde{t}_2$.

Assumption 2 (DoS Duration) [28]: There exists $\kappa_t>1$ such that

$$|\mathcal{U}(\tilde{t}_1,\tilde{t}_2)|\le(\tilde{t}_2-\tilde{t}_1)/\kappa_t \tag{21}$$

for all $t\in[\tilde{t}_1,\tilde{t}_2]$ with $0\le\tilde{t}_1<\tilde{t}_2$.

Theorem 1: Consider decay rate $\bar{\mu}>0$ with positive constants $h,\varrho_g,\kappa_t,\kappa_f$ and $\ell_g>1$. For prescribed positive parameters $\delta\in[0\ 1),\epsilon$ and γ, the filtering error system (19) utilizing the ETM in (15) is exponential stable with H_∞ attenuation lever γ, if there exist matrices $P_g>0,\Omega>0$, $Q_g>0,R_g>0$, and $U_g>0$ such that

$$\Phi_g<0, \tag{22}$$
$$P_{3-g}\le\mathfrak{e}_g\ell_gP_g \tag{23}$$
$$Q_{3-g}\le\ell_gQ_g \tag{24}$$
$$R_{3-g}\le\ell_gR_g \tag{25}$$
$$\begin{bmatrix}R_g & *\\ U_g^{\mathrm{T}} & R_g\end{bmatrix}\ge0 \tag{26}$$

with $g=1,2$, where

$$\Phi_g=\begin{bmatrix}\Phi_{11}^g & *\\ \Phi_{21}^g & \Phi_{22}^g\end{bmatrix}$$

$$\Phi_{11}^1=\begin{bmatrix}\Xi_{11}^1 & * & * & * & * & *\\ \Xi_{21}^1 & \Xi_{22}^1 & * & * & * & *\\ \tilde{B}^{\mathrm{T}}P_1 & 0 & -\gamma^2I & * & * & *\\ \Xi_{41}^1 & \Xi_{42}^1 & 0 & \Xi_{44}^1 & * & *\\ \Xi_{51}^1 & 0 & 0 & \Xi_{54}^1 & \Xi_{55}^1 & *\\ \Xi_{61}^1 & 0 & 0 & \Xi_{64}^1 & \Xi_{65}^1 & \Xi_{66}^1\end{bmatrix}$$

$$\Phi_{11}^2=\begin{bmatrix}\Xi_{11}^2 & * & * & *\\ \Xi_{21}^2 & \Xi_{22}^2 & * & *\\ \tilde{B}^{\mathrm{T}}P_2 & 0 & -\gamma^2I & *\\ \Xi_{41}^2 & \Xi_{42}^2 & 0 & \Xi_{44}^2\end{bmatrix}$$

$$\begin{aligned}
\Xi_{11}^g&=\mathrm{sym}\left\{P_g\tilde{A}_g+(-1)^{g+1}\varrho_gP_g\right\}+H^{\mathrm{T}}Q_gH\\
&\quad-\frac{a_g}{h}H^{\mathrm{T}}R_gH,\ \Xi_{21}^g=\frac{a_g}{h}U_gH\\
\Xi_{22}^g&=-a_gQ_g-\frac{a_g}{h}R_g,\ H=\begin{bmatrix}I & 0\end{bmatrix}\\
\Xi_{41}^g&=(2-g)C^{\mathrm{T}}\tilde{C}_g^{\mathrm{T}}P_g+\frac{a_g}{h}\left(R_g^{\mathrm{T}}-U_g^{\mathrm{T}}\right)H\\
\Xi_{42}^g&=\frac{a_g}{h}(R_g-U_g),\ a_g=e^{-2\varrho_g(2-g)h}\\
\Xi_{44}^g&=\frac{a_g}{h}(-2R_g+\mathrm{sym}\{U_g\})+(2-g)\Theta_1\\
\Theta_1&=\delta C^{\mathrm{T}}\Omega C+\epsilon C^{\mathrm{T}}C\\
\Xi_{51}^1&=\Xi_{61}^1=\tilde{C}_1^{\mathrm{T}}P_1,\ \Xi_{54}^1=\delta\Omega C,\ \Xi_{55}^1=(\delta-1)\Omega\\
\Xi_{64}^1&=-\delta\Omega C,\ \Xi_{65}^1=-\delta\Omega,\ \Xi_{66}^1=\delta\Omega-I\\
\Phi_{21}^g&=\begin{bmatrix}\Phi_{1g}{}^{\mathrm{T}} & \Phi_{2g}{}^{\mathrm{T}}\end{bmatrix}^{\mathrm{T}}\\
\Phi_{11}&=\sqrt{h}H\begin{bmatrix}\tilde{A}_1 & 0 & \tilde{B} & \tilde{C}_1C & \tilde{C}_1 & \tilde{C}_1\end{bmatrix}\\
\Phi_{12}&=\sqrt{h}H\begin{bmatrix}\tilde{A}_2 & 0 & \tilde{B} & 0\end{bmatrix}\\
\Phi_{21}&=\begin{bmatrix}\tilde{E}_1 & 0 & 0 & 0 & 0 & 0\end{bmatrix},\Phi_{22}=\begin{bmatrix}\tilde{E}_2 & 0 & 0 & 0\end{bmatrix}\\
\Phi_{22}^g&=\mathrm{diag}\left\{-R_g^{-1},-I\right\},\ \mathfrak{e}_1=e^{2(\varrho_1+\varrho_2)h},\ \mathfrak{e}_2=1\\
\bar{\mu}&=\varrho_1-\frac{1}{\kappa_t}(\varrho_1+\varrho_2)-\frac{1}{\kappa_f}\left((\varrho_1+\varrho_2)h+\ln\sqrt{\ell_1\ell_2}\right).
\end{aligned}$$

Proof: To facilitate expression, the following definition is given by:

$$\Gamma_1(t)=\left[\chi^{\mathrm{T}}(t),\chi^{\mathrm{T}}(t-h)H^{\mathrm{T}},\omega^{\mathrm{T}}(t),\psi_1^{\mathrm{T}}(t),\psi_2^{\mathrm{T}}(t),\psi_3^{\mathrm{T}}(t)\right]^{\mathrm{T}}$$
$$\Gamma_2(t)=\left[\chi^{\mathrm{T}}(t),\chi^{\mathrm{T}}(t-h)H^{\mathrm{T}},\omega^{\mathrm{T}}(t),\psi_1^{\mathrm{T}}(t)\right]^{\mathrm{T}}$$

where $\psi_1(t)=H\chi(t-\eta(t))$, $\psi_2(t)=e_{m+1}^k(t)$, and $\psi_3(t)=\vartheta(y(t-\eta(t)))$.

Construct the following piecewise Lyapunov–Krasovskii function for the filtering error system (19):

$$V(t)=V_g(t),\quad t\in\mathcal{F}_{g,m} \tag{27}$$

where

$$\begin{aligned}V_g(t)&=\chi^{\mathrm{T}}(t)P_g\chi(t)+\int_{t-h}^{t}\beta_g(s,t)\chi^{\mathrm{T}}(s)H^{\mathrm{T}}Q_gH\chi(s)ds\\&\quad+\int_{-h}^{0}\int_{t+v}^{t}\beta_g(s,t)\dot{\chi}^{\mathrm{T}}(s)H^{\mathrm{T}}R_gH\dot{\chi}(s)dsdv\end{aligned}$$

for $g\in\{1,2\}$, $\beta_g(s,t)=e^{2(-1)^g\varrho_g(t-s)}$.

Remark 5: Presently, few published filtering methods focus on periodic sampling CPSs under DoS attacks. To better analyze the joint model of the ETM and DoS attacks, we choose the piecewise Lyapunov–Krasovskii functional approach, which has been widely used in the research of CPSs under DoS attacks.

Taking the derivative of $V_1(t)$, we have

$$\begin{aligned}\dot{V}_1(t)&\le-2\varrho_1V_1(t)+2\chi^{\mathrm{T}}(t)P_1\dot{\chi}(t)\\&\quad+\chi^{\mathrm{T}}(t)\left[2\varrho_1P_1+H^{\mathrm{T}}Q_1H\right]\chi(t)\\&\quad+h\dot{\chi}^{\mathrm{T}}(t)H^{\mathrm{T}}R_1H\dot{\chi}(t)\\&\quad-e^{-2\varrho_1h}\chi^{\mathrm{T}}(t-h)H^{\mathrm{T}}Q_1H\chi(t-h)\\&\quad-e^{-2\varrho_1h}\int_{t-h}^{t}\dot{\chi}^{\mathrm{T}}(s)H^{\mathrm{T}}R_1H\dot{\chi}(s)ds.\end{aligned} \tag{28}$$

Note that

$$\begin{aligned}&-h\int_{t-h}^{t}\dot{\chi}^{\mathrm{T}}(s)H^{\mathrm{T}}R_1H\dot{\chi}(s)ds\\&=-h\int_{t-\eta(t)}^{t}\dot{\chi}^{\mathrm{T}}(s)H^{\mathrm{T}}R_1H\dot{\chi}(s)ds\\&\quad-h\int_{t-h}^{t-\eta(t)}\dot{\chi}^{\mathrm{T}}(s)H^{\mathrm{T}}R_1H\dot{\chi}(s)ds.\end{aligned} \tag{29}$$

By using the Jessen inequality, it yields that

$$\begin{aligned}&-h\int_{t-\eta(t)}^{t}\dot{\chi}^{\mathrm{T}}(s)H^{\mathrm{T}}R_1H\dot{\chi}(s)ds\\&\le-\frac{h}{\eta(t)}\left(\int_{t-\eta(t)}^{t}\dot{\chi}^{\mathrm{T}}(s)H^{\mathrm{T}}ds\right)R_1\left(\int_{t-\eta(t)}^{t}H\dot{\chi}(s)ds\right)\end{aligned} \tag{30}$$

and

$$\begin{aligned}&-h\int_{t-h}^{t-\eta(t)}\dot{\chi}^{\mathrm{T}}(s)H^{\mathrm{T}}R_1H\dot{\chi}(s)ds\\&\le-\frac{h}{\eta(t)}\left(\int_{t-h}^{t-\eta(t)}\dot{\chi}^{\mathrm{T}}(s)H^{\mathrm{T}}ds\right)R_1\left(\int_{t-h}^{t-\eta(t)}H\dot{\chi}(s)ds\right).\end{aligned} \tag{31}$$

From (30) and (31), one can obtain

$$-h\int_{t-h}^{t}\dot{\chi}^{\mathrm{T}}(s)H^{\mathrm{T}}R_1H\dot{\chi}(s)ds\le\tilde{\Gamma}^{\mathrm{T}}(t)\mathcal{M}\tilde{\Gamma}(t) \tag{32}$$

where $\tilde{\Gamma}(t)=col\{\chi(t),\ H\chi(t-\eta(t)),\ H\chi(t-h)\}$ and

$$\mathcal{M}=\begin{bmatrix}-H^{\mathrm{T}}R_1H & * & *\\ (R_1^{\mathrm{T}}-U_1^{\mathrm{T}})H & -2R_1^{\mathrm{T}}+U_1+U_1^{\mathrm{T}} & *\\ U_1^{\mathrm{T}}H & R_1^{\mathrm{T}}-U_1^{\mathrm{T}} & -R_1\end{bmatrix}.$$

From (15), one knows that the ETM in (15) is equivalent to

$$\begin{aligned}&e_{m+1}^{kT}(t)\Omega e_{m+1}^{k}(t)\\&\le\delta\left[\tilde{y}(t-\eta(t))+e_{m+1}^{k}(t)\right]^{\mathrm{T}}\Omega\left[\tilde{y}(t-\eta(t))+e_{m+1}^{k}(t)\right].\end{aligned}$$

Considering the sensor saturation in (5), we have

$$\begin{aligned}&\vartheta^{\mathrm{T}}(y(t-\eta(t)))\vartheta(y(t-\eta(t)))\\&\le\epsilon y^{\mathrm{T}}(t-\eta(t))y(t-\eta(t)).\end{aligned} \tag{33}$$

Combining (28)–(33) yields that

$$\begin{aligned}&\dot{V}_1(t)+2\varrho_1V_1(t)-\gamma^2\omega^{\mathrm{T}}(t)\omega(t)+e_f^{\mathrm{T}}(t)e_f(t)\\&\le\Gamma_1^{\mathrm{T}}(t)\tilde{\Phi}_1\Gamma_1(t)\end{aligned} \tag{34}$$

where $\tilde{\Phi}_1=\Phi_{11}^1+\Phi_{21}^{1\,\mathrm{T}}\Phi_{22}^{1\,-1}\Phi_{21}^1$.

Applying the Schur complement to (22) and combining with (34) follows that:

$$\dot{V}_1(t)+2\varrho_1V_1(t)+e_f^{\mathrm{T}}(t)e_f(t)-\gamma^2\omega^{\mathrm{T}}(t)\omega(t)\le0. \tag{35}$$

Similarly, when $g=2$, one can obtain that

$$\dot{V}_2(t)-2\varrho_2V_2(t)+e_f^{\mathrm{T}}(t)e_f(t)-\gamma^2\omega^{\mathrm{T}}(t)\omega(t)\le0. \tag{36}$$

From (35) and (36), it has

$$\begin{cases}V_1(t)\le\tilde{\beta}_1V_1\left(t_{1,m}\right),\ t\in\mathcal{F}_{1,m}\\ V_2(t)\le\tilde{\beta}_2V_2\left(t_{2,m}\right),\ t\in\mathcal{F}_{2,m}\end{cases} \tag{37}$$

for $\omega(t)=0$, $\tilde{\beta}_g=e^{2(-1)^g\varrho_g(t-t_{g,m})}$.

Considering the constraints of (23)–(25) together with the Lyapunov–Krasovskii function, one has

$$\begin{cases}V_1\left(t_{1,m}\right)\le\ell_2V_2\left(t_{1,m}^-\right)\\ V_2\left(t_{2,m}\right)\le\mathfrak{e}_1\ell_1V_1\left(t_{2,m}^-\right).\end{cases} \tag{38}$$

Combining (37) and (38) yields that

$$V(t)\le e^{\mu(t)}V(0) \tag{39}$$

for $t\in[t_{1,m},t_{2,m})$, where $\mu(t)=-2\varrho_1[(t-t_{1,m})+(t_{2,m-1}-t_{1,m-1})+\cdots+(t_{2,0}-t_{1,0})]+2\varrho_2[(t_{1,m}-t_{2,m-1})+(t_{1,m-1}-t_{2,m-2})+\cdots+(t_{1,1}-t_{2,0})]+2(\varrho_1+\varrho_2)hm+m\ln(\ell_1\ell_2)$ with $t_{1,0}=0$.

From (20) and (21), we have

$$\begin{aligned}\mu(t)&\le-2\varrho_1\left(t-\frac{t}{\kappa_t}\right)+2\varrho_2\frac{t}{\kappa_t}\\&\quad+\ 2(\varrho_1+\varrho_2)h\frac{t}{\kappa_f}+\frac{t}{\kappa_f}\ln(\ell_1\ell_2)\\&=-2\bar{\mu}t\end{aligned} \tag{40}$$

where $\bar{\mu}>0$ is defined in Theorem 1.

From (39) and (40), one can obtain

$$V(t)\le e^{-2\bar{\mu}t}V(0). \tag{41}$$

In the same way, for $t\in[t_{2,m},t_{1,m+1})$, we have

$$\begin{aligned}V(t)&\le\ell_1^{m+1}\ell_2^me^{q(t)+2(\varrho_1+\varrho_2)h(m+1)}V(0)\\&\le\mathcal{N}e^{-2\bar{\mu}t}V(0)\end{aligned} \tag{42}$$

with $q(t)=-2\varrho_1[(t_{2,m}-t_{1,m})+(t_{2,m-1}-t_{1,m-1})+\cdots+(t_{2,0}-t_{1,0})]+2\varrho_2[(t-t_{2,m})+(t_{1,m}-t_{2,m-1})+(t_{1,m-1}-t_{2,m-2})+\cdots+(t_{1,1}-t_{2,0})]$ and $\mathcal{N}=e^{\ln\ell_1+2(\varrho_1+\varrho_2)h}$.

For $\ell_g>1$, $\varrho_g>0$ with $g=1,2$, one can obtain $\mathcal{N}>1$. Then, from (41) and (42), it yields that

$$V(t)\le\mathcal{N}e^{-2\bar{\mu}t}V(0). \tag{43}$$

From (27), we have

$$V(t)\ge\iota_1\|\chi(t)\|^2,\ V_1(0)\le\iota_2\|\varsigma_0\|_h^2 \tag{44}$$

where $\iota_1=\min\{\lambda_{\min}(P_g)\}$, $\iota_2=\max\ \{\lambda_{\max}(P_g)+h\lambda_{\max}(Q_g)+(h^2/2)\lambda_{\max}R_g\}$, $\varsigma(t)$ represents the supplemental incipient condition of $\chi(t)$, $\varsigma(0)=\varsigma_0$, $||\varsigma_0||_h=\sup_{-h\le\hat{\varsigma}\le0}\{||\dot{\varsigma}(t+\hat{\varsigma})||\ ,||\varsigma(t+\hat{\varsigma})||\}$.

Considering (43) and (44), one has

$$\|\chi(t)\|<\sqrt{\frac{\mathcal{N}\iota_2}{\iota_1}}e^{-\bar{\mu}t}\|\varsigma_0\|_h. \tag{45}$$

Then, we can conclude that the system (19) is exponential stable with the decay rate $\bar{\mu}$.

For $\omega(t)\neq0$, it has

$$\begin{aligned}\sum_{i=0}^{m}\int_{t_{1,m}}^{t}&\Big[\dot{V}_g(t)-(-1)^g2\varrho_gV_g(t)+e_f^{\mathrm{T}}(t)e_f(t)\\&-\gamma^2\omega^{\mathrm{T}}(t)\omega(t)\Big]dt\le0\end{aligned} \tag{46}$$

from integrating (35) and (36) for $t\in\mathcal{F}_{g,m}$.

Let $m \to \infty$, and one can obtain

$$\int_0^\infty e_f^{\mathrm{T}}(t)e_f(t)dt \le \gamma^2 \int_0^\infty \omega^{\mathrm{T}}(t)\omega(t)dt. \tag{47}$$

Then, it can be concluded that the switched filtering error system (19) is exponentially stable with an H_∞ attenuation lever γ. The proof is completed. ■

In Theorem 1, sufficient conditions have been given to ensure the stability of the system (19). The weight matrix of the ETM and filter gains will be derived as follows.

Theorem 2: Consider decay rate $\bar{\mu} > 0$ with positive constants $h, \varrho_g, \kappa_f, \kappa_t$ and $\ell_g > 1$. For assigned positive parameters $\delta \in [0\ 1), \epsilon, \varepsilon_g$ and γ, the filtering error system (19) utilizing the ETM in (15) is exponential stable with H_∞ attenuation lever γ, if there exist matrices $P_{g1} > 0, P_{g3} > 0, \Omega > 0, Q_g > 0, R_g > 0, U_g > 0$ and matrices $P_{g2}, Y_g, \hat{A}_{fg}, \hat{B}_f, \hat{C}_{fg}$ with appropriate dimensions such that

$$\hat{\Phi}_g < 0 \tag{48}$$

$$P_{g1} - Y_g > 0 \tag{49}$$

$$\begin{bmatrix} P_{(3-g)1} - \mathfrak{e}_g\ell_g P_{g1} & * \\ W_g - \mathfrak{e}_g\ell_g Y_g & V_g - \mathfrak{e}_g\ell_g Y_g \end{bmatrix} \le 0 \tag{50}$$

$$Q_{3-g} \le \ell_g Q_g \tag{51}$$

$$R_{3-g} \le \ell_g R_g \tag{52}$$

$$\begin{bmatrix} R_g & * \\ U_g^{\mathrm{T}} & R_g \end{bmatrix} \ge 0 \tag{53}$$

with $g = 1, 2$, where

$$\hat{\Phi}^g = \begin{bmatrix} \hat{\Phi}_{11}^g & * \\ \hat{\Phi}_{21}^g & \hat{\Phi}_{22}^g \end{bmatrix}$$

$$\hat{\Phi}_{11}^1 = \begin{bmatrix} \hat{\Xi}_{11}^1 & * & * & * & * & * & * \\ \hat{\Xi}^1 & \hat{\Xi}_Y^1 & * & * & * & * & * \\ \hat{\Xi}_{21}^1 & 0 & \Xi_{22}^1 & * & * & * & * \\ B^{\mathrm{T}}P_{11} & B^{\mathrm{T}}Y_1 & 0 & -\gamma^2 I & * & * & * \\ \hat{\Xi}_{41}^1 & \hat{\Xi}_B^1 & \Xi_{42}^1 & 0 & \Xi_{44}^1 & * & * \\ \hat{\Xi}_{51}^1 & \hat{\Xi}_{52}^1 & 0 & 0 & \Xi_{54}^1 & \Xi_{55}^1 & * \\ \hat{\Xi}_{61}^1 & \hat{\Xi}_{62}^1 & 0 & 0 & \Xi_{64}^1 & \Xi_{65}^1 & \Xi_{66}^1 \end{bmatrix}$$

$$\hat{\Phi}_{11}^2 = \begin{bmatrix} \hat{\Xi}_{11}^2 & * & * & * & * \\ \hat{\Xi}^2 & \hat{\Xi}_Y^2 & * & * & * \\ \hat{\Xi}_{21}^2 & 0 & \Xi_{22}^2 & * & * \\ B^{\mathrm{T}}P_{21} & B^{\mathrm{T}}Y_2 & 0 & -\gamma^2 I & * \\ \hat{\Xi}_{41}^2 & 0 & \Xi_{42}^2 & 0 & \Xi_{44}^2 \end{bmatrix}$$

$$\hat{\Xi}_{11}^g = Q_g + \mathrm{sym}\left\{(-1)^{g+1}\varrho_g P_{g1} + P_{g1}A\right\} - \frac{a_g}{h}R_g$$

$$\hat{\Xi}^g = Y_g A + \hat{A}_{fg}^{\mathrm{T}} + \mathrm{sym}\left\{(-1)^{g+1}\varrho_g Y_g\right\}$$

$$\hat{\Xi}_Y^g = \mathrm{sym}\left\{(-1)^{g+1}\varrho_g Y_g + \hat{A}_{fg}\right\}$$

$$\hat{\Xi}_{21}^g = \frac{a_g}{h}U_g^{\mathrm{T}}, \hat{\Xi}_{41}^g = (2-g)C^{\mathrm{T}}\hat{B}_f^{\mathrm{T}} + \frac{a_g}{h}\left(R_g^{\mathrm{T}} - U_g^{\mathrm{T}}\right)$$

$$\hat{\Xi}_{51}^1 = \hat{\Xi}_{52}^1 = \hat{\Xi}_{61}^1 = \hat{\Xi}_{62}^1 = \hat{B}_f^{\mathrm{T}}, \hat{\Xi}_B^1 = C^{\mathrm{T}}\hat{B}_f^{\mathrm{T}}$$

$$\hat{\Phi}_{21}^g = \begin{bmatrix} \hat{\Phi}_{1g}^{\mathrm{T}} & \hat{\Phi}_{2g}^{\mathrm{T}} \end{bmatrix}^{\mathrm{T}}, \hat{\Phi}_{22}^g = \mathrm{diag}\left\{-2\varepsilon_g I + \varepsilon_g^2 R_g, -I\right\}$$

$$\hat{\Phi}_{11} = \sqrt{h}\begin{bmatrix} A & 0 & 0 & B & 0 & 0 & 0 \end{bmatrix}$$

$$\hat{\Phi}_{12} = \sqrt{h}\begin{bmatrix} A & 0 & 0 & B & 0 \end{bmatrix}$$

$$\hat{\Phi}_{21} = \begin{bmatrix} E & -\hat{C}_{f1} & 0 & 0 & 0 & 0 & 0 \end{bmatrix}$$

$$\hat{\Phi}_{22} = \begin{bmatrix} E & -\hat{C}_{f2} & 0 & 0 & 0 \end{bmatrix}$$

and the other parameters definition can be found in Theorem 1. Besides, the gains of the filter can be calculated by

$$\begin{cases} A_{fg} = P_{g2}^{-1}\hat{A}_{fg}P_{g2}^{-T}P_{g3} \\ B_f = P_{12}^{-1}\hat{B}_f \\ C_{fg} = \hat{C}_{fg}P_{g2}^{\mathrm{T}}P_{g3}. \end{cases} \tag{54}$$

Proof: Define $P_g = \begin{bmatrix} P_{g1} & P_{g2} \\ * & P_{g3} \end{bmatrix} > 0$ and matrix $Y_g = P_{g2}P_{g3}^{-1}P_{g2}^{\mathrm{T}}$. Utilizing the Schur complement to P_g, we can conclude that (49) is equal to $P_g > 0$.

Considering (23) follows that:

$$\begin{bmatrix} P_{(3-g)1} - \mathfrak{e}_g\ell_g P_{g1} & * \\ P_{(3-g)2}^{\mathrm{T}} - \mathfrak{e}_g\ell_g P_{g2}^{\mathrm{T}} & P_{(3-g)3} - \mathfrak{e}_g\ell_g P_{g3} \end{bmatrix} \le 0. \tag{55}$$

Define $Z_g = \mathrm{diag}\{I, P_{g2}P_{g3}^{-1}\}$, $W_g = P_{g2}P_{g3}^{-1}P_{(3-g)2}^{\mathrm{T}}$, and $V_g = P_{g2}P_{g3}^{-1}P_{(3-g)3}P_{g3}^{-1}P_{g2}^{\mathrm{T}}$. Pre- and post-multiplying (55) with Z_g and its transpose, we can achieve that (50) holds.

Notice that $(\varepsilon_g R_g - I)R_g^{-1}(\varepsilon_g R_g - I) \ge 0$ for $R_g > 0$ and $\varepsilon_g > 0$. Then, it follows that:

$$-R_g^{-1} \le -2\varepsilon_g I + \varepsilon_g^2 R_g. \tag{56}$$

Define $\varPi_1 = \mathrm{diag}\{Z_1, I, I, I, I, I, I, I\}$, $\varPi_2 = \mathrm{diag}\{Z_2, I, I, I, I, I\}$ and pre- and post-multiply (22) with $\varPi_g$ and its transpose. Then considering (56) yields that (48) holds with $\hat{A}_{fg} = P_{g2}A_{fg}P_{g3}^{-1}P_{g2}^{\mathrm{T}}$, $\hat{B}_f = P_{12}B_f$, and $\hat{C}_{fg} = C_{fg}P_{g3}^{-1}P_{g2}^{\mathrm{T}}$. The filter parameters in (54) can be calculated by the method in [23]. This ends the proof. ■

IV. Simulation

In this section, an illustration of the quarter-vehicle SS with the parameters in [39] is considered to validate the effectiveness of the proposed method, and the road disturbance is borrowed from [40]. The state-space realization of the SS is shown as follows:

$$A = \begin{bmatrix} 0 & 0 & 1 & -1 \\ 0 & 0 & 0 & 1 \\ -\frac{k_s}{m_s} & 0 & -\frac{c_s}{m_s} & \frac{c_s}{m_s} \\ \frac{k_s}{m_u} & -\frac{k_t}{m_u} & \frac{c_s}{m_u} & -\frac{c_s+c_t}{m_u} \end{bmatrix}, B = \begin{bmatrix} 0 \\ -1 \\ 0 \\ \frac{c_t}{m_u} \end{bmatrix},$$

$$E = \begin{bmatrix} 0 & 0 & 1 & 0 \end{bmatrix}^{\mathrm{T}}, C = \begin{bmatrix} -\frac{k_s}{m_s} & 0 & -\frac{c_s}{m_s} & \frac{c_s}{m_s} \end{bmatrix}.$$

Choose $h = 0.01$, $\delta = 0.1$, $\ell_1 = \ell_2 = 1.01$, $\kappa_t = 3.5$, $\kappa_f = 2$, $\varrho_1 = 0.1$, $\varrho_2 = 0.2$, $\epsilon = 0.16$, $\gamma = 13.5$, and $\varepsilon_1 = \varepsilon_2 = 0.2$. Utilizing Theorem 2, we have the weight matrix $\Omega = 0.1206$ and the filter gains as follows:

$$A_{f1} = \begin{bmatrix} -1.8871 & 2.7704 & 0.8080 & -0.7135 \\ -6.7515 & 18.5105 & -0.6521 & 1.7672 \\ -38.1031 & -14.2420 & -2.6669 & 2.6404 \\ 372.9579 & -895.2162 & 28.7592 & -34.3737 \end{bmatrix}$$

$$A_{f2} = \begin{bmatrix} -1.8871 & 2.7704 & 0.8080 & -0.7135 \\ -6.7515 & 18.5105 & -0.6521 & 1.7672 \\ -38.1031 & -14.2420 & -2.6669 & 2.6404 \\ 372.9579 & -895.2162 & 28.7592 & -34.3737 \end{bmatrix}$$

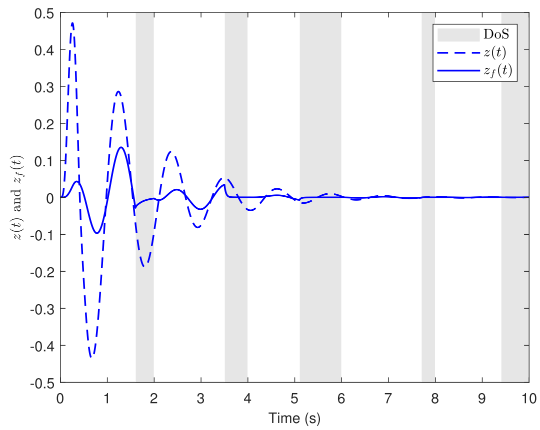

Fig. 4. Trajectories of $z(t)$ and $z_f(t)$ in case i).

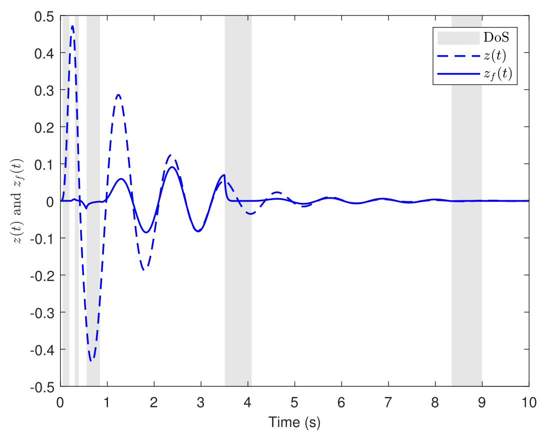

Fig. 5. Trajectories of $z(t)$ and $z_f(t)$ in case ii).

$$C_{f1} = \begin{bmatrix} 0.0127 & -0.0505 & -0.9974 & -0.0050 \end{bmatrix}$$
$$C_{f2} = \begin{bmatrix} 0.0044 & -0.0100 & -0.9986 & -0.0004 \end{bmatrix}$$
$$B_f = \begin{bmatrix} 0.0171 & 0.0128 & 0.0071 & -0.1580 \end{bmatrix}^{\mathrm{T}}.$$

To verify the effectiveness of our proposed method, the following two cases of randomly generated DoS attacks will be studied.

Case i): DoS attacks are generated randomly over the simulation duration, which are given by $\mathcal{A}_1(0, 10) = \{[1.600 - 1.998], [3.500 - 3.991], [5.100 - 5.441], [5.449 - 5.996], [7.700 - 8.000], [9.400 - 9.999]\}$, and intervals of VDAs are $\bar{\mathcal{A}}_1(0, 10) = \{[1.600 - 2.000], [3.500 - 4.000], [5.100 - 6.000], [7.700 - 8.000], [9.400 - 10.000]\}$.

Case ii): DoS attacks are mainly active in the transient stage of the SS under disturbance, which are given by $\mathcal{A}_2(0, 10) = \{[0.040 - 0.111], [0.116 - 0.198], [0.300 - 0.398], [0.550-0.849], [3.500-4.090], [8.340-8.999]\}$, and intervals of VDAs are $\bar{\mathcal{A}}_2(0, 10) = \{[0.040-0.200], [0.300-0.400], [0.550 - 0.850], [3.500 - 4.090], [8.340 - 9.000]\}$.

Figs. 4–11 show simulation results for the filtering error SS using the proposed communication strategy. In Figs. 4 and 5, the blue dotted line represents the output of the SS measured by the sensor, and the blue line denotes the output of the filter under the road disturbance. Figs. 6 and 7 are the filtering error in case i) and case ii), respectively. It can be seen from

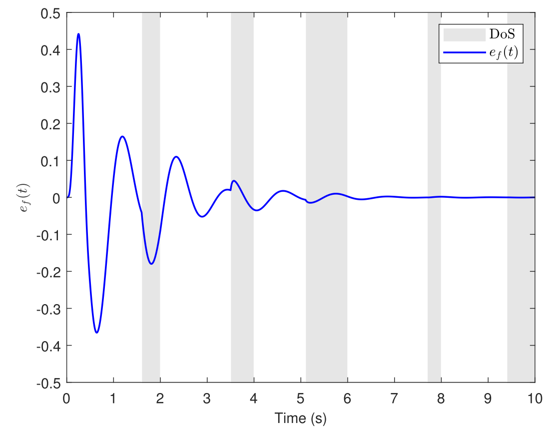

Fig. 6. Filtering error in case i).

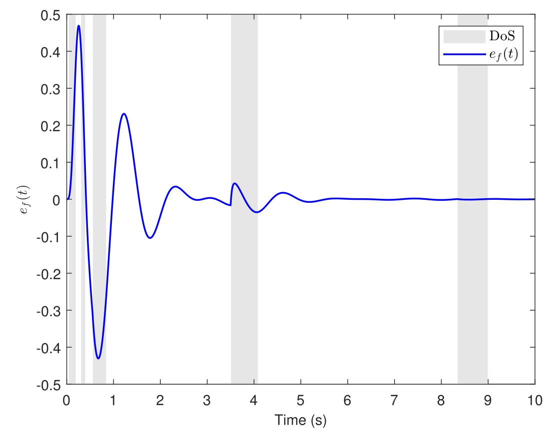

Fig. 7. Filtering error in case ii).

Figs. 4 and 5 that DoS attacks affect the performance of the designed filter, in the same time interval of 0.55–0.85 s, the filtering performance of case i) during sleep periods of DoS attacks is significantly better than that of case ii). However, from Figs. 6 and 7, one can conclude that the system's output can be well estimated during sleep periods of DoS attacks by using the proposed method such as 0.85–3.5 s in case ii).

Compared to the estimation signals $z(t)$, $z_f(t)$ and estimation error $e(t)$ of the SS under nonperiodic DoS attacks in Fig. 5 and [31, Fig. 6], the system's output can be better estimated during sleep periods of DoS attacks by using the proposed method in this article. Besides, different from the measured output in [31] is unsprung mass velocity, the measurement output of this article selects the acceleration of sprung mass, which is easier to be measured by sensors in reality.

In Figs. 8 and 9, the blue line, black line, red dotted line, and magenta dashed dotted line represent the actual output of the estimated SS $y(h_i)$, filter input $y_f(t)$, measurement output with the sensor saturation $\tilde{y}(h_i)$, and the threshold of the sensor saturation $\bar{y}$ under VDAs, respectively. The threshold of the sensor saturation $\bar{y}$ is 2.600 $\mathrm{m/s^2}$ and the maximum amplitude of output $|y_i(t)|$ max is 4.190 $\mathrm{m/s^2}$. Then, it yields that $(1 - [\bar{y}/|y(t)| \max])^2 \approx 0.144 < \epsilon$.

From Figs. 8 and 9, one can obtain that the input of the filter is zero under the active period of VDAs. Figs. 10 and 11

TABLE I
NSTP, NTP, NDS, AND ADRR IN CASE I)

time (s)	0-1.60	1.60-2.00 (VDA)	2.00-3.50	3.50-4.00 (VDA)	4.00-5.10	5.10-6.00 (VDA)	6.00-7.70	7.70-8.00 (VDA)	8.00-9.40	9.40-10.00 (VDA)
NSTP	49	1	34	1	28	1	44	1	37	1
NTP	49	40	34	50	28	90	44	30	37	60
NDS	160	40	150	50	110	90	170	30	140	60
ADRR	30.63%	2.50%	22.67%	2.00%	25.45%	1.11%	25.88%	3.33%	26.43%	1.67%

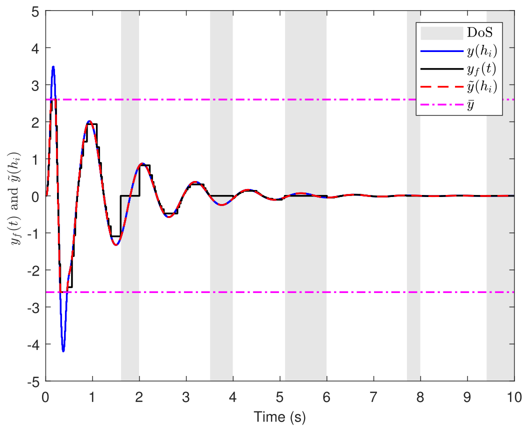

Fig. 8. State responses in case i).

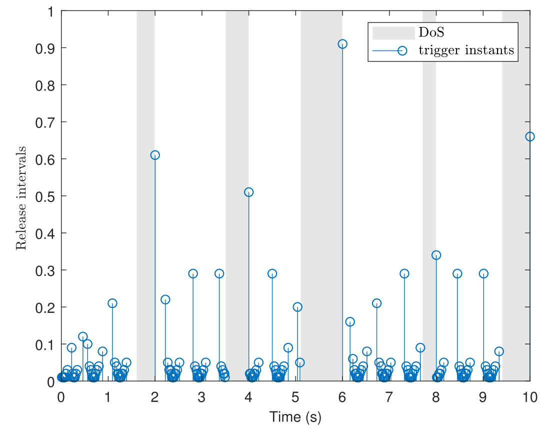

Fig. 10. Release instants under DoS attacks in case i).

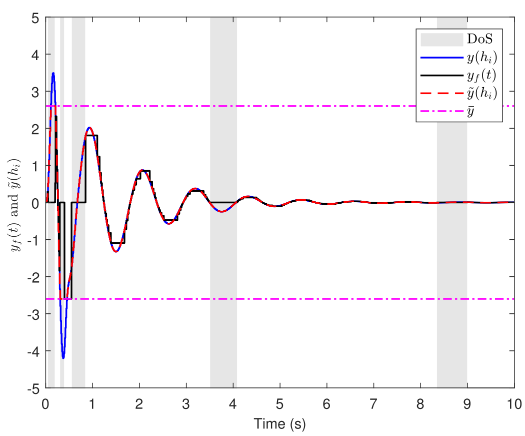

Fig. 9. State responses in case ii).

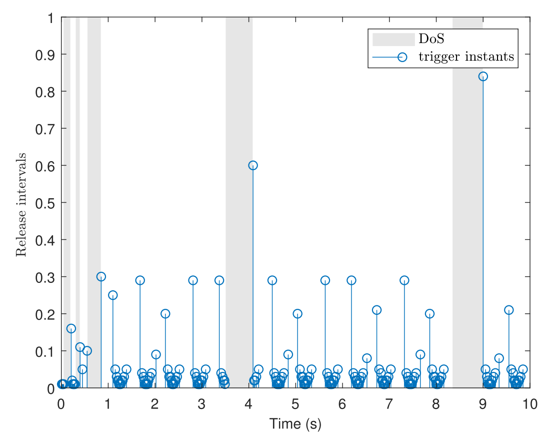

Fig. 11. Release instants under DoS attacks in case ii).

depict the valid release intervals under VDAs. Also, from Figs. 8–11, one can see that the filter cannot achieve packets under the active periods of VDAs. However, based on the communication strategy we proposed, the latest packet containing the measurement of the SS can be successfully transmitted over the network after the end of VDA, such as the packet in 2 s under case i) in Fig. 10, which can ensure the filter performance.

To better validate the effectiveness of the designed communication strategy considering the ETM and DoS attacks, we first define the average data releasing rate (ADRR), the number of successfully transmitted packets (NSTPs), the number of data sampling (NDS), and the number of triggered packets (NTPs), where ADRR = (NSTP/NDS). Statistical results in case i) and case ii) are listed in Tables I and II. From Table I, we can conclude that the NDS is 1000, the NSTP is 197, and the ADRR is 19.70% in 10 s under case i) and the NDS is 1000, the NSTP is 214 and the ADRR is 21.40% in 10 s under case ii), which implies that the burden of network bandwidth is significantly reduced. Besides, during the active period of VDAs, the ETM continues to form the periodical transmission attempts, and the latest measurement output of the SS can be successfully transmitted via the network at the end of the VDA, for example, the NSPT is 1 and the NTP is 40 within the active period of the VDA 1.6–2.0 s in case i). From Tables I and II, it can be obtained that the ADRR during the road disturbance period is greater than that in other periods in DoS sleep periods, which means that more data packets are released by using our proposed method to ensure the filter performance during the road disturbance period.

TABLE II
NSTP, NTP, NDS, AND ADRR IN CASE II)

time (s)	0-0.04	0.04-0.20 (VDA)	0.20-0.30	0.30-0.40 (VDA)	0.40-0.55	0.55-0.85 (VDA)	0.85-3.50	3.50-4.09 (VDA)	4.09-8.34	8.34-9.00 (VDA)	9.00-10.00
NSTP	4	1	8	1	2	1	63	1	104	1	28
NTP	4	16	8	10	2	30	63	159	104	66	28
NDS	4	16	10	10	15	30	265	159	425	66	100
ADRR	100 %	6.25%	80%	10.00%	13.33%	3.33%	23.77%	0.62%	24.47%	1.52%	28%

V. CONCLUSION

In this article, we have investigated the problem of H_∞ filtering for CPSs with the sensor saturation against DoS attacks. A new ETM considering DoS attacks has been developed to relieve the burden of the network and ensure the filter performance under DoS attacks. The challenging problem that the end of the DoS attack occurs at the sampling period is addressed by defining the VDA model and using the periodical transmission attempt method. Sufficient conditions for CPSs with the proposed communication strategy are derived based on the piecewise Lyapunov–Krasovskii approach. Finally, an illustrative example of the quarter-vehicle SS has been presented to manifest the effectiveness of the proposed filter design approach. We will focus on designing the joint model with some state-of-the-art ETMs and DoS attacks, such as memory ETM and dynamic ETM for future research.

REFERENCES

[1] Y. Li, L. Shi, P. Cheng, J. Chen, and D. E. Quevedo, "Jamming attacks on remote state estimation in cyber-physical systems: A game-theoretic approach," *IEEE Trans. Autom. Control*, vol. 60, no. 10, pp. 2831–2836, Oct. 2015.

[2] X. Ge, Q.-L. Han, M. Zhong, and X.-M. Zhang, "Distributed krein space-based attack detection over sensor networks under deception attacks," *Automatica*, vol. 109, Nov. 2019, Art. no. 108557.

[3] D. Du, C. Zhang, H. Wang, X. Li, H. Hu, and T. Yang, "Stability analysis of token-based wireless networked control systems under deception attacks," *Inf. Sci.*, vol. 459, pp. 168–182, Aug. 2018.

[4] J. Cao, D. Ding, J. Liu, E. Tian, S. Hu, and X. Xie, "Hybrid-triggered-based security controller design for networked control system under multiple cyber attacks," *Inf. Sci.*, vol. 548, pp. 69–84, Feb. 2021.

[5] D. Ding, Q.-L. Han, Y. Xiang, X. Ge, and X.-M. Zhang, "A survey on security control and attack detection for industrial cyber-physical systems," *Neurocomputing*, vol. 275, pp. 1674–1683, Jan. 2018.

[6] Y. Yang, D. Yue, and C. Dou, "Output-based event-triggered schemes on leader-following consensus of a class of multi-agent systems with Lipschitz-type dynamics," *Inf. Sci.*, vol. 459, pp. 327–340, Aug. 2018.

[7] Z. Gu, C. K. Ahn, D. Yue, and X. Xie, "Event-triggered H_∞ filtering for T–S fuzzy-model-based nonlinear networked systems with multisensors against DoS attacks," *IEEE Trans. Cybern.*, vol. 52, no. 6, pp. 5311–5321, Jun. 2022.

[8] S. Hu, D. Yue, X. Yin, X. Xie, and Y. Ma, "Adaptive event-triggered control for nonlinear discrete-time systems," *Int. J. Robust Nonlinear Control*, vol. 26, no. 18, pp. 4104–4125, Dec. 2016.

[9] D. Yue, J. Fang, and S. Won "Delay-dependent robust stability of stochastic uncertain systems with time delay and Markovian jump parameters," *Circuits Syst. Signal Process.*, vol. 22, no. 4 pp. 351–365, Jul. 2003.

[10] Y. Yang, D. Yue, and Y. Xue, "Decentralized adaptive neural output feedback control of a class of large-scale time-delay systems with input saturation," *J. Franklin Inst.*, vol. 352 no. 5, pp. 2129–2151, May 2015.

[11] H. Yan, H. Zhang, F. Yang, X. Zhan, and C. Peng, "Event-triggered asynchronous guaranteed cost control for Markov jump discrete-time neural networks with distributed delay and channel fading," *IEEE Trans. Neural Netw. Learn. Syst.*, vol. 29, no. 8, pp. 3588–3598, Aug. 2018.

[12] H. Fawzi, P. Tabuada, and S. Diggavi, "Secure estimation and control for cyber-physical systems under adversarial attacks," *IEEE Trans. Autom. Control*, vol. 59, no. 6, pp. 1454–1467, Jun. 2014.

[13] L. Liu and X. Li, "Event-triggered tracking control for active seat suspension systems with time-varying full-state constraints," *IEEE Trans. Syst., Man, Cybern., Syst.*, vol. 52, no. 1, pp. 582–590, Jan. 2022.

[14] S. Yan, M. Shen, S. K. Nguang, and G. Zhang. "Event-triggered H_∞ control of networked control systems with distributed transmission delay," *IEEE Trans. Autom. Control*, vol. 65, no. 10, pp. 4295–4301, Oct. 2020.

[15] E. Tian and D. Yue, "Reliable H_∞ filter design for T–S fuzzy model-based networked control systems with random sensor failure," *Int. J. Robust Nonlinear Control*, vol. 23, no. 1, pp. 15–32, Jan. 2013.

[16] H. Wang, P. Shi, and J. Zhang, "Event-triggered fuzzy filtering for a class of nonlinear networked control systems," *Signal Process.*, vol. 113, pp. 159–168, Aug. 2015.

[17] J. Cao, Z. Bu, Y. Wang, H. Yang, J. Jiang, and H.-J. Li, "Detecting prosumer-community groups in smart grids from the multiagent perspective," *IEEE Trans. Syst., Man, Cybern., Syst.*, vol. 49, no. 8, pp. 1652–1664, Aug. 2019.

[18] S. H. You, C. K. Ahn, S. Zhao, and Y. S. Shmaliy, "Frobenius norm-based unbiased finite impulse response fusion filtering for wireless sensor networks," *IEEE Trans. Ind. Electron.*, vol. 69, no. 2, pp. 1867–1876, Feb. 2022.

[19] S. Liu, Z. Wang, G. Wei, and M. Li, "Distributed set-membership filtering for multirate systems under the Round-Robin scheduling over sensor networks," *IEEE Trans. Cybern.*, vol. 50, no. 5, pp. 1910–1920, May 2020.

[20] D. Yue, E. Tian, and Q.-L. Han, "A delay system method for designing event-triggered controllers of networked control systems," *IEEE Trans. Autom. Control*, vol. 58, no. 2, pp. 475–481, Feb. 2013.

[21] Z. Ye, D. Zhang, Z.-G. Wu, and H. Yan, "A3C-based intelligent event-triggering control of networked nonlinear unmanned marine vehicles subject to hybrid attacks," *IEEE Trans. Intell. Transp. Syst.*, vol. 23, no. 8, pp. 12921–12934, Aug. 2022.

[22] H. Zhang, X. Zheng, H. Yan, C. Peng, Z. Wang, and Q. Chen, "Codesign of event-triggered and distributed H_∞ filtering for active semi-vehicle suspension systems," *IEEE/ASME Trans. Mechatronics*, vol. 22, no. 2, pp. 1047–1058, Apr. 2017.

[23] Z. Gu, P. Shi, D. Yue, and Z. Ding, "Decentralized adaptive event-triggered H_∞ filtering for a class of networked nonlinear interconnected systems," *IEEE Trans. Cybern.*, vol. 49, no. 5, pp. 1570–1579, May 2019.

[24] E. Tian and C. Peng, "Memory-based event-triggering H_∞ load frequency control for power systems under deception attacks," *IEEE Trans. Cybern.*, vol. 50, no. 11, pp. 4610–4618, Nov. 2020.

[25] C. Deng, D. Zhang, and G. Feng, "Resilient practical cooperative output regulation for MASs with unknown switching exosystem dynamics under DoS attacks," *Automatica*, vol. 139, May 2022, Art. no. 110172.

[26] P. Chen, D. Zhang, L. Yu, and H. Yan, "Dynamic event-triggered output feedback control for load frequency control in power systems with multiple cyber attacks," *IEEE Trans. Syst., Man, Cybern., Syst.*, vol. 52, no. 10, pp. 6246–6258, Oct. 2022.

[27] X. Yin, Z. Gao, D. Yue, and S. Hu, "Cloud-based event-triggered predictive control for heterogeneous NMASs under both DoS attacks and transmission delays," *IEEE Trans. Syst., Man, Cybern., Syst.*, early access, Mar. 28, 2022, doi: 10.1109/TSMC.2022.3160510.

[28] C. De Persis and P. Tesi, "Input-to-state stabilizing control under denial-of-service," *IEEE Trans. Autom. Control*, vol. 60, no. 11, pp. 2930–2944, Nov. 2015.

[29] S. Hu, D. Yue, X. Xie, X. Chen, and X. Yin, "Resilient event-triggered controller synthesis of networked control systems under periodic DoS jamming attacks," *IEEE Trans. Cybern.*, vol. 49, no. 12, pp. 4271–4281, Dec. 2019.

[30] J. Liu, T. Yin, J. Cao, D. Yue, and H. R. Karimi, "Security control for T–S fuzzy systems with adaptive event-triggered mechanism and multiple cyber-attacks," *IEEE Trans. Syst., Man, Cybern., Syst.*, vol. 51, no. 10, pp. 6544–6554, Oct. 2021.

[31] S. Hu, D. Yue, X. Chen, Z. Cheng, and X. Xie, "Resilient H_∞ filtering for event-triggered networked systems under nonperiodic DoS jamming attacks," *IEEE Trans. Syst., Man, Cybern., Syst.*, vol. 51, no. 3, pp. 1392–1403, Mar. 2021.

[32] L. Ma, Z. Wang, and H.-K. Lam, "Event-triggered mean-square consensus control for time-varying stochastic multi-agent system with sensor saturations," *IEEE Trans. Autom. Control*, vol. 62, no. 7, pp. 3524–3531, Jul. 2017.

[33] J. Hu, Z. Wang, and H. Gao, "Joint state and fault estimation for time-varying nonlinear systems with randomly occurring faults and sensor saturations," *Automatica*, vol. 97, pp. 150–160, Nov. 2018.

[34] X. Bu, Z. Hou, Q. Yu, and Y. Yi, "Quantized data driven iterative learning control for a class of nonlinear systems with sensor saturation," *IEEE Trans. Syst., Man, Cybern., Syst.*, vol. 50, no. 12, pp. 5119–5129, Dec. 2020.

[35] H. Dong, Z. Wang, and H. Gao, "Fault detection for Markovian jump systems with sensor saturations and randomly varying nonlinearities," *IEEE Trans. Circuits Syst. I, Reg. Papers*, vol. 59, no. 10, pp. 2354–2362, Oct. 2012.

[36] V. Nithya, R. Sakthivel, and Y. Ren, "Resilient H_∞ filtering for networked nonlinear Markovian jump systems with rand omly occurring distributed delay and sensor saturation," *Nonlinear Anal. Model. Control*, vol. 26, no. 2, pp. 187–206, Mar. 2021.

[37] M. J. Lacerda, "Filter design for continuous-time linear systems subject to sensor saturation," *Math. Probl. Eng.*, vol. 2017, pp. 1–8, Jul. 2017.

[38] L. Sun, Y. Wang, and G. Feng "Control design for a class of affine nonlinear descriptor systems with actuator saturation," *IEEE Trans. Autom. Control*, vol. 60, no. 8, pp. 2195–2200, Aug. 2015.

[39] X. Ge and Q.-L. Han, "Distributed event-triggered H_∞ filtering over sensor networks with communication delays," *Inf. Sci.*, vol. 291, pp. 128–142, Jan. 2015.

[40] Z. Gu, S. Fei, Y. Zhao, and E. Tian, "Robust control of automotive active seat-suspension system subject to actuator saturation," *J. Dyn. Syst. Meas. Control*, vol. 136, no. 4, Jul. 2014, Art. no. 41022.

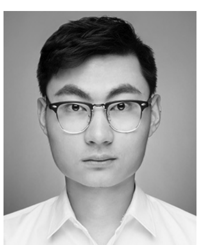

Xiang Sun received the B.S. degree in vehicle engineering from the Jiangsu University of Technology, Changzhou, China, in 2017, and the M.S. degree in control science and engineering from Nanjing Forestry University, Nanjing, China, in 2019, where he is currently pursuing the Ph.D. degree in control science and engineering.

He is currently a visiting Ph.D. student with the Department of Electrical Engineering, Yeungnam University, Gyeongsan, South Korea. His current research interests include suspension systems, event-triggered control, and secure control.

Zhou Gu (Member, IEEE) received the B.S. degree in automation from North China Electric Power University, Beijing, China, in 1997, and the M.S. and Ph.D. degrees in control science and engineering from the Nanjing University of Aeronautics and Astronautics, Nanjing, China, in 2007 and 2010, respectively.

From September 1999 to January 2013, he was with the School of Power Engineering, Nanjing Normal University, Nanjing, as an Associate Professor. He is currently a Professor with Nanjing Forestry University, Nanjing. His current research interests include networked control systems, time-delay systems, reliable control, and their applications.

Dong Yue (Fellow, IEEE) received the Ph.D. degree in engineering from the South China University of Technology, Guangzhou, China, in 1995.

He is currently a Professor and the Dean of the Institute of Advanced Technology for Carbon Neutrality, Nanjing University of Posts and Telecommunications, Nanjing, China, and also a Changjiang Professor with the Department of Control Science and Engineering, Huazhong University of Science and Technology, Wuhan, China. Up to now, he has published more than 100 papers in international journals. His research interests include analysis and synthesis of networked control systems, multiagent systems, optimal control of power systems, and Internet of Things.

Prof. Yue is currently an Associate Editor of the IEEE Control Systems Society Conference Editorial Board and was an Associate Editor of the IEEE TRANSACTIONS ON INDUSTRIAL INFORMATICS, *IEEE Industrial Electronics Magazine*, IEEE TRANSACTIONS ON SYSTEMS, MAN, AND CYBERNETICS—PART A: SYSTEMS AND HUMANS, and IEEE TRANSACTIONS ON NEURAL NETWORKS AND LEARNING SYSTEMS from 2016 to 2018.

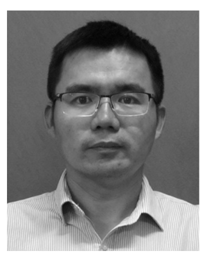

Xiangpeng Xie (Member, IEEE) received the B.S. degree in thermal automation and the Ph.D. degree in engineering from Northeastern University, Shenyang, China, in 2004 and 2010, respectively.

From 2012 to 2014, he was a Postdoctoral Fellow with the Department of Control Science and Engineering, Huazhong University of Science and Technology, Wuhan, China. He is currently a Professor with the Institute of Advanced Technology, Nanjing University of Posts and Telecommunications, Nanjing, China. His research interests include fuzzy modeling and control synthesis, state estimations, optimization in process industries, and intelligent optimization algorithms.